Flexure of steel bridge deck plate with asphalt surfacing

Flexure of Steel Bridge Deck Plate with Asphalt Surfacing

Flexion de tablier de pont métallique avec un revêtement asphaltique

Biegung von Stahlfahrbahnplatten mit Asphalt-Belag

M. S. G. CULLIMORE
Reader
University of Bristol,
Bristol, England

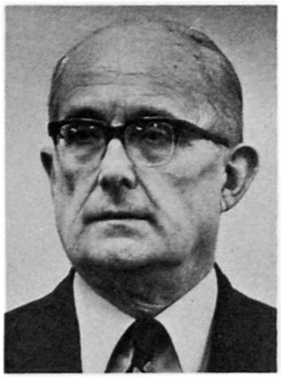

M. Stuart Cullimore, born 1920, graduated in civil engineering from Bristol University in 1940. Now Reader in Structural Engineering. His research in recent years has been on fatigue of structural joints and bridge decks.

I. D. FLETT
Research Student
University of Bristol,
Bristol, England

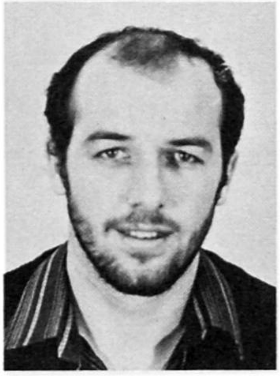

Innes Flett, born 1958, is a graduate of the University of Aberdeen with a degree in engineering. For the past 3 years he has been investigating local stresses induced in surfaced bridge decks at the University of Bristol.

J. W. SMITH
Lecturer
University of Bristol,
Bristol, England

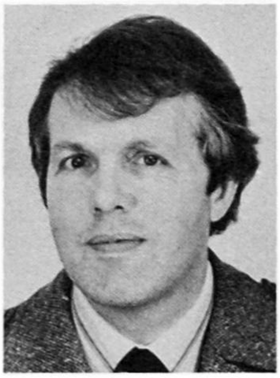

John William Smith, born 1941, studied at the Univ. of Edinburgh, Scotland. He obtained a Ph.D. at the Univ. of Bristol (on bridge vibrations), has been a Lecturer in the Dep. of Civil Engineering since 1968.

SUMMARY

The partial interaction between a steel bridge deck plate and its asphalt road surface is discussed. The problem, including slip in the flexible tack coat interface, was reduced to the flexure of a 3-layer beam and analysed by an Airy stress function method. Good agreement was obtained with experiments and finite element analysis. The solution was used to obtain effective moduli for asphalt and tack coat material from dynamic beam tests and the use of these data to predict the response of samples with different properties is demonstrated.

RÉSUMÉ

L'influence réciproque d'un tablier de pont métallique et d'une couche de roulement en asphalte sur leur comportement respectif est présenté. Le problème, comportant le glissement dans la couche souple d'asphalte, a été ramené à la flexion d'une poutre à trois lamelles et étudié par la méthode des contraintes à l'aide d'une fonction d'Airy. Une bonne concordance a pu être constatée entre les résultats d'essai et l'analyse au moyen des éléments finis. La solution livre des modules effectifs pour l'asphalte et le matériau de collage à partir des essais dynamiques de la poutre et ces valeurs permettent de prédire le comportement de différentes éprouvettes.

ZUSAMMENFASSUNG

Die partielle Interaktion zwischen einer Stahlfahrbahnplatte und dem Asphalt-Belag wird diskutiert. Das Problem, einschliesslich der Gleitungen in der flexiblen Zwischenschicht, wurde als Biegung eines dreilamelligen Balkenmodells unter Verwendung der Airy'schen Spannungsfunktion behandelt. Es wurde eine gute Übereinstimmung zwischen Experiment und der Berechnung mit Hilfe finiter Elemente erhalten. Die Lösung wurde verwendet, um aus dynamischen Balkenversuchen die wirksamen Module für Asphalt und Zwischenschicht zu erhalten und das Verhalten von Proben mit anderen Eigenschaften vorauszusagen.

1. INTRODUCTION

The preferred form of construction of light steel roadway decks for long span bridges is shown in Fig. 1. This consists typically of a 12 mm deckplate stiffened by V-shaped steel troughs spanning, in the direction of traffic flow, between cross girders or box diaphragms. The deck plate is usually surfaced with mastic asphalt with a thin bituminous tack coat bonding the two materials together.

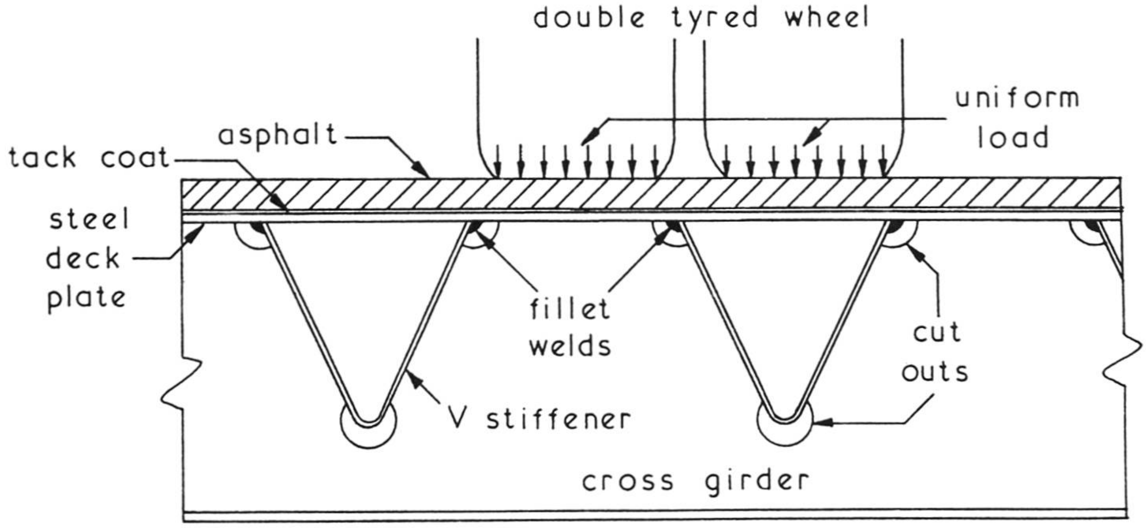

Fig.1. Orthotropic Steel Bridge Construction

This, so called, orthotropic deck is a flexible structure which is highly sensitive to the local bending action produced by the wheel loads of heavy commercial vehicles. The bridge deck can be expected to suffer many millions of cycles of wheel loading during its life, so that fatigue is an important design criterion, especially for details such as the longitudinal deck plate to stiffener fillet weld. The resistance to fatigue of the asphalt surfacing is also important, bearing in mind the need to maximise the interval between the costly and disruptive re-surfacing operations.

An analysis of bare steel decks by Cullimore and Smith [1] gave results which compared well with laboratory measurements on a full size panel. It was realised, however, that surfacing modifies the stress distribution by spreading the wheel load over a larger area as compared with the bare steel deck and also by acting structurally with it. The importance of asphalt in reducing the steel stresses under moving loads was noted by the Transport and Road Research Laboratory [2] , but lack of a satisfactory quantification of the composite action has allowed advantage of the load spreading effect only to be taken in design.

Asphalt is a visco-elastic material so that the stress analysis for moving loads is a dynamic problem. Its properties are also significantly temperature dependent. A further complication is the slip that occurs in the tack coat layer [3].

It has, however, been demonstrated that [4] for normal vehicle speeds the problem may be treated as a static one in terms of effective elastic stiffness moduli. These were shown to be most satisfactorily obtained from deflections and strains measured in dynamic beam tests on steel plates surfaced with the asphalt together with the appropriate tack coat. Given a method of analysis of the composite action, effective stiffness moduli for both asphalt and tack coat may be determined for the required range of operating temperatures. These data may then be used in design to predict deflections and stresses in both the steel and asphalt for other steel plate and asphalt thickness combinations within these ranges.

2. COMPOSITE ACTION THEORIES

A natural simplification is to take a transverse slice of surfaced plate and treat it as a beam problem. This then would be similar to the partial interaction problem in steel/concrete composite construction where there is some slip at the interface resisted elastically by the shear connectors. The solution offered by Johnson [5] assumes that both steel and concrete components have the same radius of curvature (hence no separation) and plane cross-sections before and after loading. This produces the strain diagram shown in Fig. 2a. However, experiments reported later in this paper reveal a strain distribution that is not compatible with these assumptions. This is shown in Fig. 2b and the significant difference is that the strain in the asphalt increases less rapidly with depth than does the corresponding strain in the steel.

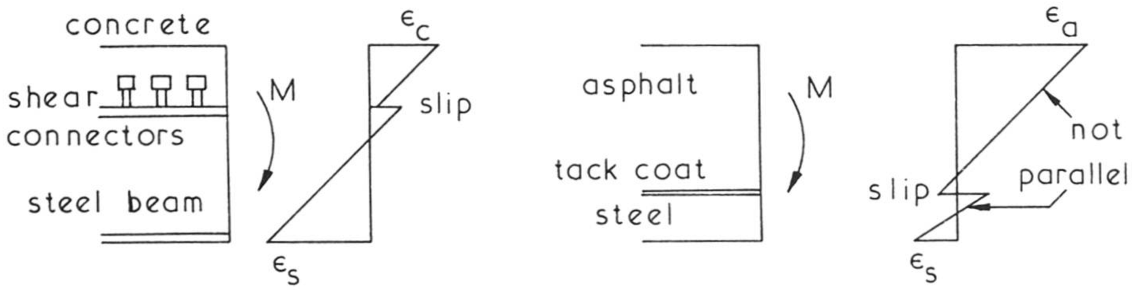

(a) Composite Construction (b) Steel/Asphalt Plates

Fig.2. Strain Distribution with Partial Interaction

Similar theories for bending of sandwich beams and plates have been offered by di Taranto [6,7]. These have adopted essentially the same assumptions as Johnson and therefore do not model accurately the observed behaviour which is considered to be caused by shear lag in the asphalt and consequently warping of the cross-section.

The analysis of a multi-layer elastic beam was tacked by Rao [8] using Airy stress functions. This seemed to be the most promising approach and was adopted for the particular problem of bending in steel plates with asphalt surfacing. It has already been pointed out that the question of viscoelasticity in the asphalt may be dealt with by considering the material to have an effective elastic stiffness at a fixed temperature and loading speed. Thus the problem may be reduced to a 2-layer beam connected by a thin interface layer of elastic shear stiffness.

The solution of the problem by Airy stress functions is presented here and compared with a 2-dimensional finite element analysis together with some experimental results.

3. ANALYSIS BY AIRY STRESS FUNCTION

The maximum tensile stress in the asphalt - critical for fatigue life estimation - occurs when a double tyred vehicle wheel straddles a trough edge as shown in Fig. 1. The hogging moment corresponds to the conditions at the root of a suitably loaded cantilever. The specific problem to be analysed is therefore the 2-layer cantilever, of unit width, with elastic interface shown in Fig. 3 subjected to an end load, P. Coordinates x, y and x, η for the asphalt and steel components respectively are also shown in the figure. For convenience the thicknesses d_1 and d_2 are often expressed in terms of their respective half thicknesses h_1 and h_2.

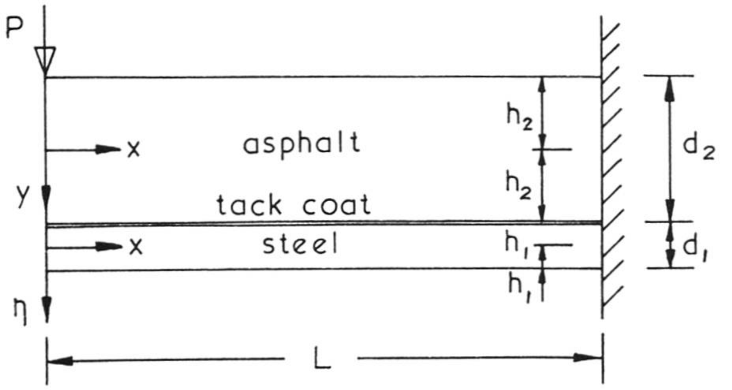

Fig.3. Two Layer Cantilever with Elastic Interface

The solution of two dimensional problems in elasticity [9], in the absence of body forces, reduces to the integration of the equation

$$\frac{\partial^4\phi}{\partial x^4} + 2\frac{\partial^4\phi}{\partial x^2\partial y^2} + \frac{\partial^4\phi}{\partial y^4} = 0$$

where ϕ is a stress function such that

$$\sigma_x = \frac{\partial^2\phi}{\partial y^2}, \quad \sigma_y = \frac{\partial^2\phi}{\partial x^2}, \quad \tau_{xy} = -\frac{\partial^2\phi}{\partial x\partial y}$$

having regard to boundary conditions. Stress functions in the form of polynomials of the third degree were found to be suitable. Thus for the asphalt

$$\phi_a = \frac{\alpha}{6}xy^3 + \beta xy + \frac{\gamma}{2}xy^2$$

and for the steel

$$\phi_s = \frac{a}{6}x\eta^3 + bx\eta + \frac{c}{2}x\eta^2$$

These satisfy the differential equation and may be differentiated to give the stresses in the asphalt

$$\sigma_x = \alpha xy + \gamma x, \quad \sigma_y = 0, \quad \tau_{xy} = -\frac{\alpha}{2}y^2 - \beta - \gamma y$$

and in the steel

$$\sigma_x = ax\eta + cx, \quad \sigma_\eta = 0, \quad \tau_{x\eta} = -\frac{a}{2}\eta^2 - b - c\eta$$

To make top and bottom edges free of shear stress

$$-\frac{\alpha}{2}h_2^2 - \beta + \gamma h_2 = 0 \qquad (1)$$

$$-\frac{a}{2}h_1^2 - b - ch_1 = 0 \qquad (2)$$

For shear stress compatibility at interface

$$-\frac{\alpha}{2}h_2^2 - \beta - \gamma h_2 = -\frac{a}{2}h_1^2 - b - ch_1 \qquad (3)$$

To satisfy the loaded end condition the shearing forces integrated over this end must be equal to P. Hence

$$P = -\int_{-h_2}^{h_2} \tau_{xy}\, dy - \int_{-h_1}^{h_1} \tau_{x\eta}\, d\eta$$

$$= \frac{\alpha}{2} I_2 + \beta d_2 + \frac{a}{2} I_1 + bd_1 \qquad (4)$$

where I_1 and I_2 are the second moments of area of the steel and asphalt cross sections.

The full solution of the problem requires the displacement compatibility at the interface to be considered. The displacements may be obtained by integrating the strains. The strains in the asphalt, for example, are given by

$$\varepsilon_x = \frac{\partial u}{\partial x} = \frac{\sigma_x}{E} = \frac{\alpha}{E} xy + \frac{\gamma}{E} x$$

$$\varepsilon_y = \frac{\partial v}{\partial y} = -\frac{\nu}{E}\sigma_x = -\frac{\nu}{E}(\alpha xy + \gamma x)$$

$$\gamma_{xy} = \frac{\partial u}{\partial y} + \frac{\partial v}{\partial x} = \frac{\tau_{xy}}{G} = -\frac{1}{G}\left(\frac{\alpha}{2}y^2 + \beta + \gamma y\right)$$

It should be noted, in passing, that $\frac{\partial \varepsilon_x}{\partial y} = \frac{\alpha}{E} x$ so that the longitudinal direct strain in the asphalt varies linearly with depth as, similarly does the corresponding strain in the steel.

Integration of these equations yields the displacement components

$$u = \frac{1}{E}\left(\frac{\alpha}{2} x^2 y + \frac{\gamma}{2} x^2\right) + \left(\frac{\nu}{E} - \frac{1}{G}\right)\left(\frac{\alpha}{6} y^3 + \frac{\gamma}{2} y^2\right) + dy + h$$

$$v = -\frac{\nu}{E}\left(\frac{\alpha}{2} xy^2 + \gamma xy\right) - \frac{\alpha}{6E} x^3 + ex + g$$

where e, d, h and g are constants of integration and $e + d = -\frac{\beta}{G}$

The constants of integration are determined by the constraint conditions at the support; $x = L$, $y = 0$. At this point u and v will both be zero. Hence

$$0 = \frac{\gamma L^2}{2E} + h \quad \text{and} \quad 0 = -\frac{\alpha L^3}{6E} + eL + g$$

It will have been observed from the previous equations that the cross section of the beam is distorted. Thus the chosen stress function results in two possibilities for the conditions at the fixed end. These are illustrated in

Fig. 4. In fact the fixed end is not free to distort and the conditions would thus be different from either of those shown. However, condition (a) corresponds with the usually assumed shear deflection behaviour of beams and was preferred after comparison of both conditions with the finite element analysis in the next section.

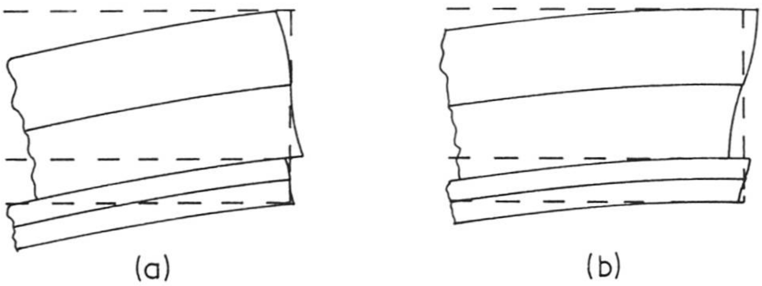

Fig.4. Two Possible Conditions at Fixed End

Condition (a) is given by

$$\left(\frac{\partial u}{\partial y}\right) = 0 \text{ at } x = L \text{ and } y = 0$$

Hence $$0 = \frac{\alpha L^2}{2E} + d$$

From these constraint conditions the constants e, d, h and g may be obtained thus giving explicit expressions for the displacement components thus:

$$u = \frac{1}{E}\left(\frac{\alpha}{2}\,x^2 y + \frac{\gamma}{2}\,x^2\right) - \frac{(2+\nu)}{E}\left(\frac{\alpha}{6}\,y^3 + \frac{\gamma}{2}\,y^2\right) - \frac{\alpha L^2}{2E}\,y - \frac{\gamma L^2}{2E}$$

$$v = -\frac{\nu}{E}\left(\frac{\alpha}{2}\,xy^2 + \gamma xy\right) - \frac{\alpha x^3}{6E} + \frac{\alpha L^2}{2E}\,x + \frac{2\beta(1+\nu)(L-x)}{E} - \frac{\alpha L^3}{3E}$$

Similar expressions exist for the displacement components in the steel but with y replaced by η and stress function coefficients a, b and c instead of α, β and γ.

For displacement compatibility at the interface two conditions are assumed:

(a) The slopes of the asphalt and steel are identical at the interface assuming that the tack coat layer is very thin. This may be expressed as

$$\left(\frac{dv_a}{dx}\right)_{y\,=\,h_2} = \left(\frac{dv_s}{dx}\right)_{\eta\,=\,-h_1}$$

where subscripts a and s are used to denote asphalt and steel respectively. Hence

$$-\frac{\nu_a}{E_a}\left(\frac{\alpha}{2}\,h_2^2 + \gamma h_2\right) - \frac{\alpha x^2}{2E_a} + \frac{\alpha L^2}{2E_a} - \frac{2\beta(1+\nu_a)}{E_a}$$

$$= -\frac{\nu_s}{E_s}\left(\frac{a}{2}\,h_1^2 - ch_1\right) - \frac{ax^2}{2E_s} + \frac{aL^2}{2E_s} - \frac{2b(1+\nu_s)}{E_s} \qquad (5)$$

(b) There is an elastic slippage at the interface

$$S_i = (u_a)_{y = h_2} - (u_s)_{\eta = -h_1}$$

such that $S_i = -\frac{\tau_i}{\kappa_i}$

where τ_i = interface shear stress

κ_i = interface shear stiffness

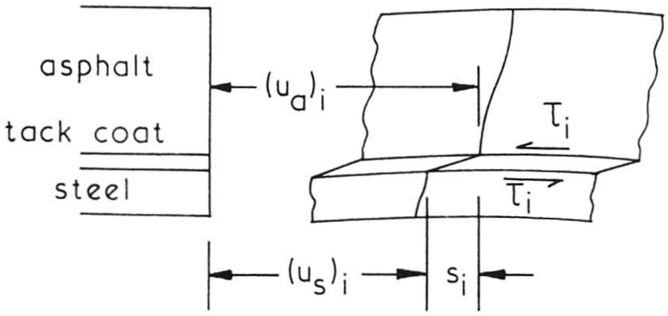

Fig.5. Elastic Shear Slip at Interface

This condition is illustrated in Fig. 5. The direction of shear stress shown is determined by the usual sign convention. Thus

$$\frac{\alpha}{2} h_2^2 + \beta + \gamma h_2 = \kappa_i \left\{ \frac{1}{E_a}\left(\frac{\alpha}{2} x^2 h_2 + \frac{\gamma}{2} x^2\right) - \frac{(2+\nu_a)}{E_a}\left(\frac{\alpha}{6} h_2^3 + \frac{\gamma}{2} h_2^2\right) - \frac{\alpha L^2}{2E_a} h_2 - \frac{\gamma L^2}{2E_a} - \frac{1}{E_s}\left(- \frac{a}{2} x^2 h_1 + \frac{c}{2} x^2\right) + \frac{(2+\nu_s)}{E_s}\left(- \frac{a}{6} h_1^3 + \frac{c}{2} h_1^2\right) - \frac{aL^2}{2E_s} h_1 + \frac{cL^2}{2E_s} \right\} \quad (6)$$

The equations(1) to (6) are therefore used to determine the six constants α, β, γ and a, b, c in the formulae for the stress functions. An explicit solution of the equations is possible in the form

$$\alpha = \frac{A_3B_2 - B_3A_2}{A_1B_2 - A_2B_1}, \quad a = \frac{B_3A_1 - A_3B_1}{A_1B_2 - A_2B_1}$$

$$\beta = \frac{1}{D}\left[\alpha\left(I_2 - \frac{D}{2} h_2^2\right) + aI_1 + P\right]$$

$$b = \frac{1}{D}\left[\alpha I_2 + a\left(I_1 - \frac{D}{2} h_1^2\right) + P\right]$$

$$\gamma = \frac{1}{Dh_2}(\alpha I_2 + aI_1 + P)$$

$$c = -\frac{h_2}{h_1}\gamma$$

where

$$A_1 = -\mu I_2(2 + 3\nu_a) + I_2(2 + 3\nu_s) + \frac{\mu D h_2^2}{2}(2 + \nu_a) + \frac{\mu D L^2}{2}$$

$$A_2 = -\mu I_1(2 + 3\nu_a) + I_1(2 + 3\nu_s) - \frac{Dh_1^2}{2}(2 + \nu_s) - \frac{DL^2}{2}$$

$$A_3 = P\,[\,\mu(2 + 3\nu_a) - (2 + 3\nu_s)\,]$$

$$B_1 = \frac{2E_sI_2}{\kappa_i} + (2 + \nu_a)\frac{\mu h_2}{2}(\frac{h_2^2D}{2} + I_2) + \frac{L^2}{2}(\mu h_2D + \frac{\mu I_2}{h_2} + \frac{I_2}{h_1}) + (2 + \nu_s)\frac{h_1}{2}I_2$$

$$B_2 = \frac{2E_sI_1}{\kappa_i} + (2 + \nu_a)\frac{\mu h_2}{2}I_2 + \frac{L^2}{2}(\frac{\mu I_1}{h_2} + h_1D + \frac{I_1}{h_1}) + (2 + \nu_s)\frac{h_1}{2}(\frac{h_1^2D}{3} + I_1)$$

$$B_3 = -P\,[\,\frac{2E_s}{\kappa_i} + (2 + \nu_a)\frac{\mu h_2}{2} + \frac{L^2}{2}(\frac{\mu}{h_2} + \frac{1}{h_1}) + (2 + \nu_s)\frac{h_1}{2}\,]$$

$$D = 2(h_1 + h_2) = \text{depth of beam}$$

$$\mu = E_s/E_a = \text{modular ratio}$$

It has been remarked above that the strain varies less rapidly with depth in the asphalt than in the steel, as shown in Fig. 2b. For this to be so

$$\frac{\partial\varepsilon_a}{\partial y} \Big/ \frac{\partial\varepsilon_s}{\partial\eta} < 1$$

But from the formula obtained for the stresses

$$\frac{\partial\varepsilon_a}{\partial y} \Big/ \frac{\partial\varepsilon_s}{\partial\eta} = \frac{\partial\sigma_a}{E_a\partial y} \Big/ \frac{\partial\sigma_s}{E_s\partial\eta} = \frac{\alpha x}{E_a} \Big/ \frac{ax}{E_s} = \mu\frac{\alpha}{a}$$

Hence it is required that

$$\mu\,(\frac{A_3B_2 - B_3A_2}{B_3A_1 - A_3B_1}) < 1$$

The following numerical values are considered to be representative for practical purposes:

$$E_s = 200{,}000\ \text{N/mm}^2\ ,\quad \mu = 20\ ,\quad \nu_s = 0.3\ ,\quad \nu_a = 0.4$$

$$\kappa_i = 400\ \text{N/mm}^2\ ,\quad P = 1\text{N}$$

$$L = 100\ \text{mm}\ ,\quad h_1 = 5\ \text{mm}\ ,\quad h_2 = 20\ \text{mm}$$

Substituting these values in the previous formula it is found that

$$\mu\frac{\alpha}{a} = 0.698 < 1$$

This verifies that the experimental observations are caused by a shear lag effect in the asphalt.

4. FINITE ELEMENT ANALYSIS

The stress function solution was compared with a finite element analysis of the configuration. The mesh required 340 elements of which 300 were in the steel and asphalt and were of dimensions 5 mm x 3.2 mm. The remaining 40 elements were of dimensions 5 mm x 0.5 mm and were required to simulate the 1 mm thick tack coat layer at the interface. Four noded 2-dimensional elements were adopted.

The deflected form of the structure is shown in Fig. 6. Two features of the behaviour should be noted. Firstly, because the tack coat layer is a rubberised bitumen and of lower modulus that the asphalt, there is significant elastic shear deformation in it. Secondly, the pronounced warping of the asphalt cross section may be clearly observed. It is this warping, due to shear lag, that results in the asphalt strain being less than would be deduced from the assumption of plane cross-sections adopted in previous analyses of the partial interaction problem.

The deflections calculated by the stress function solution are compared with the finite element analysis in Fig. 7. The deflection profiles are compared at the mid-depth of the asphalt and mid-depth of the steel. The small discrepancies should be attributed to the difference between the assumed condition of fixity (Fig. 4a) and the true conditions. The assumption of Fig. 4b was also considered but compared less favourably. The strain distribution at a cross section 25 mm from the fixed end is shown in Fig. 8. Again the agreement is very good though the finite element analysis reveals slightly greater shear lag in the asphalt. The very narrow elements used to represent the tack coat layer may not, however, give wholly satisfactory results there as may be seen in the figure.

5. EXPERIMENTAL METHOD

The critical loading condition for producing maximum tensile stress in the asphalt is when a double tyred vehicle wheel straddles the trough edge as depicted in Fig. 1. Experimentally, this was simulated by loading a beam-like sample in 3-point bending using the arrangement shown in Fig. 9 which provided for reversal of load.

The beam was supported over a span of 300 mm using a system of T pieces screwed to the steel plate connected by strips of spring steel to a channel section reaction frame. The spring steel strips acted effectively as simple supports giving negligible resistance to bending. A servo controlled hydraulic jack produced an upward force designated as positive. The dimensions of the sample were as shown and four strain gauges were attached, one on the upper asphalt surface, one on the lower steel surface and two on the side of the specimen, one on either side of the interface.

Because asphalt is viscoelastic it has mechanical stiffness that depends on both speed of loading and temperature. The speed of loading was represented by a dynamic impulse corresponding to a particular frequency controlled by the servo jack. As asphalt is very sensitive to temperature variation particularly in the region of 20°C, it was imperative to maintain a constant temperature during testing. The sample and loading frame were enclosed within a chamber in which it was possible to control temperatures over a range from -20°C to +50°C with a tolerance of ±0.5°C for these impulse load tests.

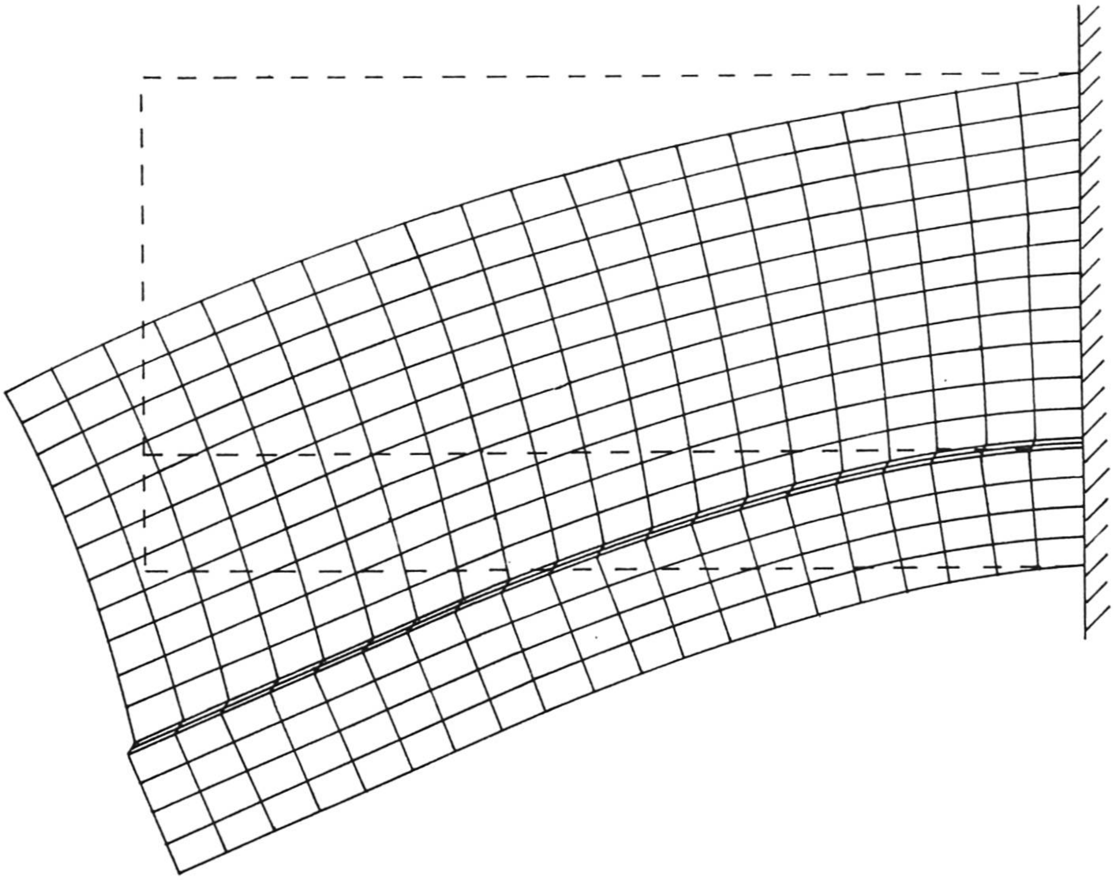

Fig.6. Finite Element Analysis - Deflections

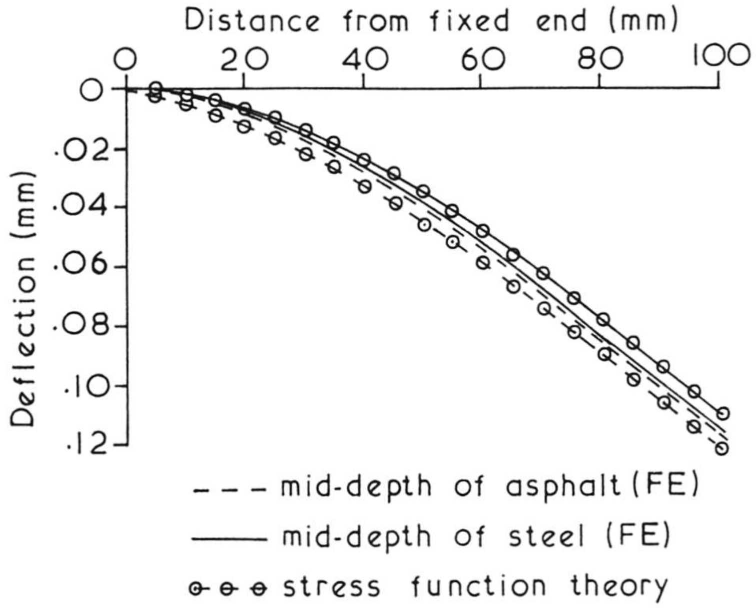

Fig.7. Deflection - Comparison of Finite Element with Stress Function

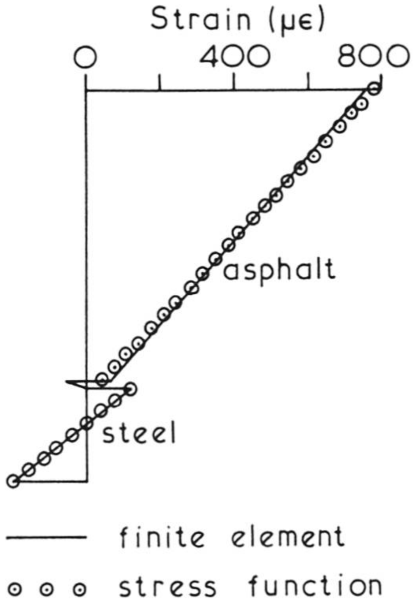

Fig.8. Strain Distribution 25 mm from Fixed End

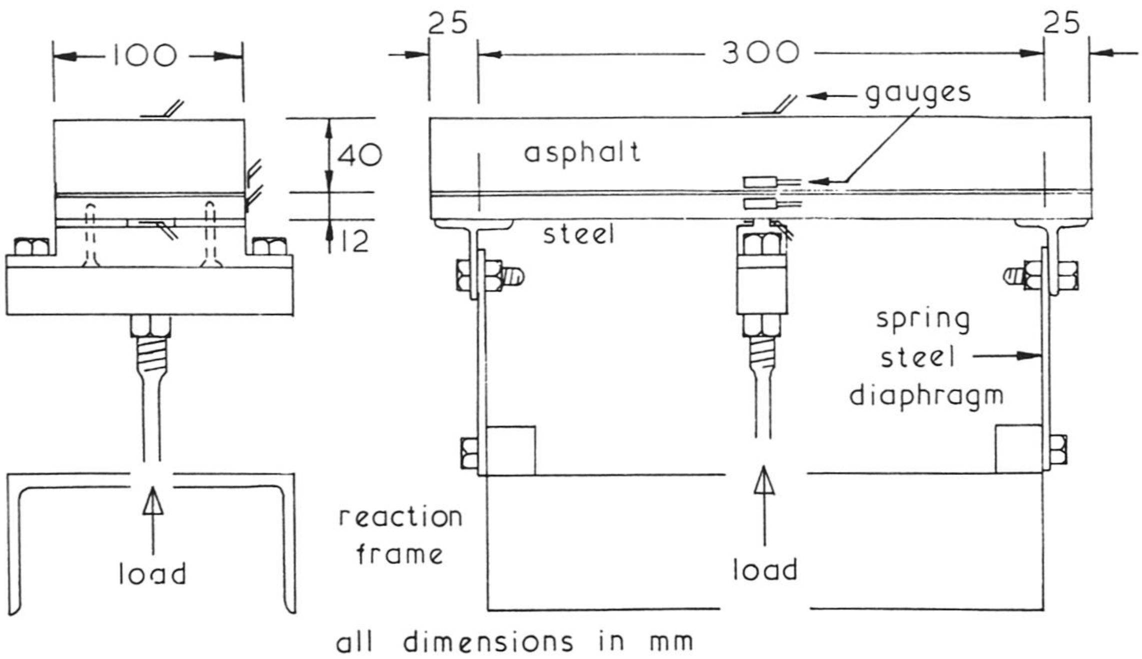

Fig.9. Experimental Configuration

6. DISCUSSION OF RESULTS

Strains observed experimentally are shown in Fig. 10 and are compared with those calculated by the stress function theory. The agreement is very good at all three temperatures and confirms the significance of the shear lag in the asphalt.

The values of stiffness modulus of both asphalt and tack coat, which gave the best fit to the experimental results, are tabulated in Table 1 for the three chosen temperatures. It may be observed that the tack coat stiffness modulus is always an order of magnitude less than that of the asphalt.

Loading Frequency = 50 Hz

Young's modulus of steel = 201.4 GN/m^2

Temperature ^{o}C	Stiffness (GN/m^2)	
	Asphalt	Tack Coat
0	17.0	0.6
20	6.4	0.1
35	0.92	0.01

Table 1. Calculated Stiffnesses of Asphalt and Tack Coat

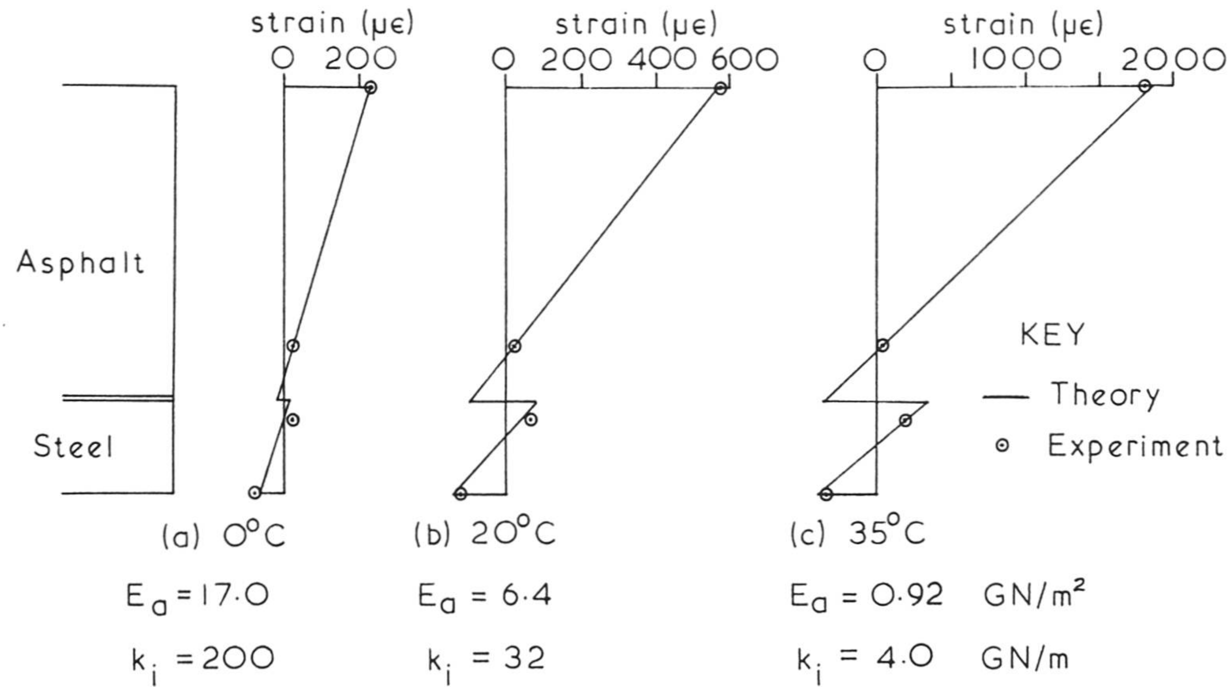

Fig.10. Experimental Strains Compared with Stress Function Theory

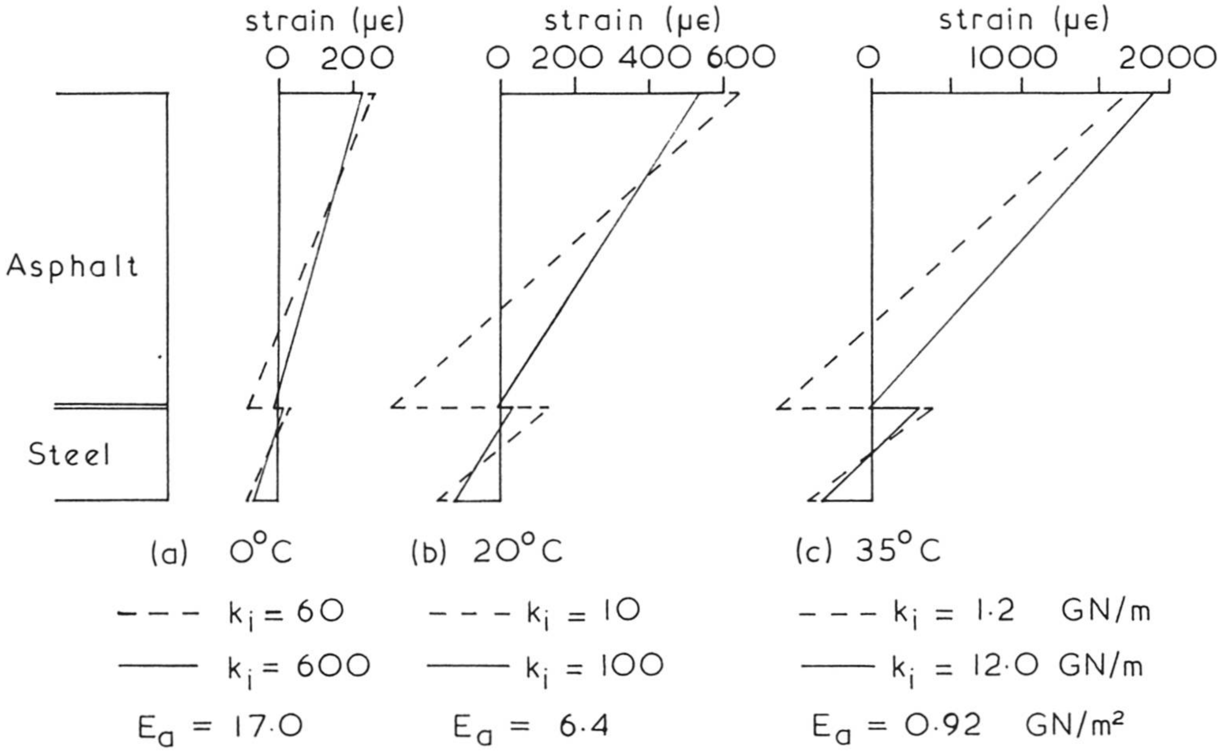

Fig.11. Effect of Variation in Tack Coat Stiffness

To illustrate the practical use of the theory presented here, the effect of varying the stiffness of the tack coat on its own will now be considered.

At each temperature the tack coat stiffness was varied from approximately one third to three times the stiffness found in the tests. Thus in Fig. 11 the strain distributions are plotted showing the effects of a ten-fold change in tack coat stiffness. The most significant effect is the change in slip at the interface where the softest tack coat results in much reduced interaction between steel and asphalt. It had been hoped that by using a stiff tack coat and thereby increasing the interaction it would be possible to reduce the maximum tensile stress in the asphalt. Figs. 11a and 11b show this to be so at 0°C and 20°C but, as can be seen in Fig. 11c, not at 35°C. In neither case, however, is the decrease significant.

The method may also be used to investigate the effect of varying the asphalt thickness. This is done in Fig. 12 where the thickness is varied from 25 mm to 45 mm. There is a significant increase in asphalt strain when the thickness is reduced at temperatures of 0°C and 20°C. However, at 35°C there is very little overall change with a slight reduction at 25 mm. Thus, since asphalt fatigue depends on the number of repetitions at a particular maximum strain, there might be a case for reducing the thickness of the paving with consequent economy, especially for bridges where there is a high average road surface temperature.

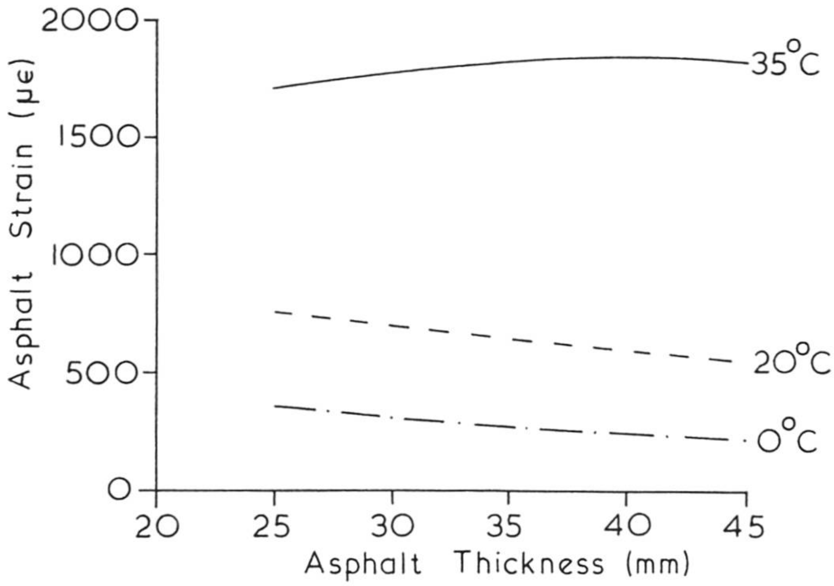

Fig.12. Effect of Variation in Asphalt Thickness

7. CONCLUSIONS

A theory has been presented to describe the behaviour of steel bridge deck plate surfaced with asphalt and a thin flexible tack coat interface. This theory enables asphalt and tack coat stiffness moduli to be determined from simple beam tests. These data enable the effect of partial composite action to be accounted for in the design of beams with any combination of steel plate and asphalt thickness.

The experimental observation of shear lag in the asphalt was confirmed by the theory and found to be of significant magnitude in the range of test parameters considered. The tack coat interface layer was found to be very much less stiff than the asphalt itself. Changing the stiffness of the tack coat relative to the asphalt was investigated and was found to radically alter the strain distribution.

A suitable plate theory for the partial interaction phenomenon is still required for the full analysis of bridge deck panels. However, the theory presented here explains the behaviour that has been observed by previous investigators, and could be used to make an appropriate two-dimensional analysis of a bridge deck panel.

8. ACKNOWLEDGEMENTS

The work described in this paper was supported jointly by the SERC and the Department of Transport as a CASE award. The authors are grateful for this support together with the interest shown by the Materials Division of the Transport and Road Research Laboratory.

9. REFERENCES

(1) CULLIMORE, M.S.G. and SMITH, J.W.: Local Stresses in Orthotropic Steel Bridge Decks Caused by Wheel Loads. Journal of Constructional Steel Research, Vol. 1, No. 2, 1981, 17-26.

(2) NUNN, D.E. and MORRIS, S.A.H.: Trials of Experimental Orthotropic Bridge Deck Panels Under Traffic Loading. Transport and Road Research Laboratory Report No. 627, Crowthorne, 1974.

(3) MORRIS, S.A.H.: Stresses Under Dynamic Wheel Loading in a Surfaced Steel Orthotropic Deck with V-Stiffeners. Transport and Road Research Laboratory Supplementary Report No. 237, Crowthorne, 1976.

(4) CULLIMORE, M.S.G. and SMITH, J.W.: Utilisation of the Structural Action of Bituminous Road Surfacing for Steel Bridge Decks. Colloquium on the Effective Use of Materials in Structures, IABSE, Imperial College, London, September 1981.

(5) JOHNSON, R.P.: Composite Structures of Steel and Concrete. Appendix A, Vol. 1, Crosby Lockwood Staples, London, 1975.

(6) DiTARANTO, R.A.: Theory of Vibratory Bending for Elastic and Viscoelastic Layered Finite-Length Beams. Journal of Applied Mechanics, Transactions of the ASME, Series E, Vol. 32, December 1965, 881-886.

(7) DiTARANTO, R.A.: Static Analysis of a Laminated Beam. Journal of Engineering for Industry, Transactions of the ASME, Series B, Vol. 95, August 1973, 755-761.

(8) RAO, K.M. and GHOSH, B.G.: Exact Analysis of Unsymmetric Laminated Beam. Proceedings of ASCE, Journal of the Structural Division, ST11, Vol. 105, November 1979, 2313-2325.

(9) TIMOSHENKO, S.P. and GOODIER, J.N.: Theory of Elasticity. McGraw Hill, New York, 1951.